Processing and Application of Ceramics 19 [3] (2025) 273–279
https://doi.org/10.2298/PAC2503273C

Phase relations in the Eu_2O_3-Fe_2O_3 system at 1300 and 1400 °C

Olga V. Chudinovych[1,*], Anatoliy V. Samelyuk[1], Serhiy F. Korichev[1], Victor S. Flis[2]

[1] *I.M. Frantsevich Institute for Problems in Materials Science NAS of Ukraine, 3, Omeliana Pritsaka St., 03142, Kyiv, Ukraine*

[2] *G. V. Kurdyumov Institute for Metal Physics NAS of Ukraine, 36 Academician Vernadsky Blvd., 03142 Kyiv, Ukraine*

Received 11 July 2025; Received in revised form 1 September 2025; Accepted 18 September 2025

Abstract

Phase relations in the Eu_2O_3-Fe_2O_3 system at 1300 and 1400 °C were studied in the whole concentration range by X-ray diffraction and scanning electron microscopy. The samples were prepared with a concentration step of 1 to 5 mol%. The samples of different compositions were prepared from nitrate acid solutions by evaporation, drying and calcinations at 1300 and 1400 °C. The isothermal cross-sections of the Eu_2O_3-Fe_2O_3 phase diagram at 1300 and 1400 °C show the presence of four single-phase regions (B-Eu_2O_3, $EuFeO_3$ (R), $Eu_3Fe_5O_{12}$ and Fe_2O_3) and three two-phase regions (B-Eu_2O_3 + $EuFeO_3$, $EuFeO_3$ + $Eu_3Fe_5O_{12}$ and $Eu_3Fe_5O_{12}$ + Fe_2O_3). The refined lattice parameters and the boundaries of the homogeneity fields for solid solutions were determined. The range of homogeneity of solid solutions based on the R-phase extends from 49 to 52 mol% Eu_2O_3 at 1300 and 1400 °C. The range of homogeneity of solid solutions based on the $Eu_3Fe_5O_{12}$ extends from 61 to 63 mol% Fe_2O_3 at 1300 and 1400 °C.

Keywords: *phase equilibria, Fe_2O_3, Eu_2O_3, perovskite, solid solutions, lattice parameters*

I. Introduction

Currently, various types of dielectric, magnetic and magneto-dielectric materials are being widely studied. In the Fe_2O_3-Eu_2O_3 oxide system, complex oxide phases such as $EuFeO_3$ and $Eu_3Fe_5O_{12}$ are formed. These compounds have significant potential for applications in spintronics, magneto-optics and sensors. $EuFeO_3$ crystallises in an orthorhombic structure like perovskite and exhibits antiferromagnetic order at room temperature with a Neel transition temperature of about 640 K [1]. This material has magnetoelectric properties and is used in spintronics. Its crystallochemical stability and ability to be doped make it promising for thin-film materials. In addition, studies have shown the ability of $EuFeO_3$ to produce photovoltaic effects under ultraviolet light [2]. $Eu_3Fe_5O_{12}$ is a rare-earth iron garnet with a cubic structure. It is characterised by high saturated magnetic induction and good magneto-optical properties, including the Faraday effect, which makes it suitable for use in optical insulators, modulators and data storage devices [3]. Substitution of Eu with other rare earth elements allows tuning the magnetic and spectral characteristics of the material for specific technological purposes.

The right choice of optimal compositions for the synthesis of materials is the key to obtain materials with the desired physical and chemical properties. The reference data for determining the optimal compositions are the equilibrium state diagrams, as they can be used to determine the region of existence of solid solutions. The Fe_2O_3-Eu_2O_3 system has been studied in detail in different works [4–11]. Ristić *et al.* [4] investigated phase transformations at Eu_2O_3:Fe_2O_3 molar ratios of 1:1 and 3:5 within the temperature range of 900–1300 °C. At 900 °C, the formation of the $EuFeO_3$ phase accompanied by residual Eu_2O_3 was observed. Increasing the temperature to 1100–1300 °C promotes the formation of a more thermodynamically stable phase, $Eu_3Fe_5O_{12}$. The thermodynamic characteristics of phase transitions in this system were reported by Sugihara *et al.* [10], who determined the standard enthalpies of formation to be −63.3 kcal/mol for $EuFeO_3$ and −297.8 kcal/mol for $Eu_3Fe_5O_{12}$. $EuFeO_3$ has an orthorhombically distorted perovskite-type structure [12–14], with unit cell param-

* Corresponding author: +86 18107739072
e-mail: *diamondcnmc@163.com*
Co-first authors: Peicheng Mo, Wenlin Yu

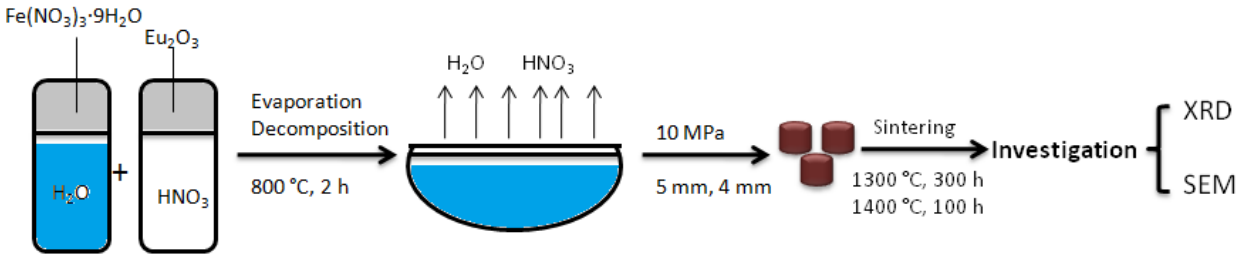

Figure 1. Scheme of synthesis and study of solid solutions of the Fe_2O_3-Eu_2O_3 system

eters: a = 5.376(7) Å, b = 5.599(5) Å, c = 7.691(2) Å; space group *Pbnm* [12].

The synthesis of a single-phase $Eu_3Fe_5O_{12}$ with a cubic garnet structure (a = 12.50369(8) Å, space group $Ia\bar{3}d$ [15]) requires either longer annealing times or higher temperatures compared to the formation of the perovskite phase [15,16]. Opuchovic *et al.* [16] have shown that after the heat treatment of a precursor gel at 1073 K, prepared using 1,2-ethanediol as a complexing agent, $EuFeO_3$ remained the dominant phase, even in the sample with a nominal composition corresponding to the garnet phase.

To date, all studies of the Fe_2O_3-Eu_2O_3 system have focused exclusively on the complex oxide phases $EuFeO_3$ and $Eu_3Fe_5O_{12}$. However, the homogeneity range of these phases has not been determined yet. This study aims to investigate the interaction between europium and iron oxides at 1300 and 1400 °C across the full compositional range and to determine the concentration intervals where the respective phases remain stable. The Fe_2O_3-Eu_2O_3 system exhibits a high propensity to form stable binary oxides with promising properties for practical applications. Further investigation of this system is relevant for the development of novel ferrite and sensor materials.

II. Experimental

Eu_2O_3 (99.99%, produced by Merck Corp.), $Fe(NO_3)_3 \cdot 9\,H_2O$ (99.99%, GOST 4111-74) and nitric acid (65%, Czech Republic) were used as starting materials.

The specimens with different concentrations of Fe_2O_3 (0, 0.5, 1, 2, 5, 15, 30, 45, 49, 50, 51, 55, 60, 63, 65, 70, 85, 90, 95 and 100 mol%) were prepared from Eu^{3+}/Fe^{3+} nitrate solutions with their subsequent evaporation and decomposition at 800 °C for 2 h (Fig. 1). Solutions of Eu^{3+} nitrates were obtained by dissolving europium oxide in nitric acid. The obtained powders were pressed at 10 MPa into pellets of 5 mm in diameter and 4 mm in height. To study phase relationships at 1300 and 1400 °C thermal treatment of the as-prepared samples was carried out in two stages: at 1100 °C (for 100 h in air) and then at 1300 °C (for 300 h in air) or at 1400 °C (for 100 h in air) in the furnaces with heating elements based on Fecral (H23U5T) and Superkanthal ($MoSi_2$), respectively. The heating rate was 3 °C/min.

Characterization of the samples was carried out using physicochemical methods X-ray diffraction (XRD) and electron microscopy (SEM). For phase composition analysis, X-ray patterns were obtained on an X-ray diffractometer DRON-3M (Burevestnik, Leningrad; CuKα radiation with a nickel filter). The scan rate was 0.05–0.1 °°/min in the range 2θ = 15–80°. Lattice parameters were refined by least squares fitting using the LATTIC program. The effective precision of the measurements was ±0.0002 nm. Scanning electron microscopy (Superprobe-733, JEOL, Japan, Palo Alto, CA) was used to assess the homogeneity of the samples. Elemental analysis of the samples was performed by X-ray spectral microanalysis (XMR) using an energy dispersive spectrometer (EDS) INCA 450 (OXFORD Instruments).

III. Results and discussion

The chemical and phase compositions in the Eu_2O_3-Fe_2O_3 system annealed at 1300 and 1400 °C with lattice constants are summarized in Table 1 and Table 2, respectively. The results were used to plot the isothermal section of the Eu_2O_3-Fe_2O_3 phase diagram at 1300 and 1400 °C (Fig. 2).

According to SEM and XRD analyses there were Eu_2O_3, Fe_2O_3, $Eu_3Fe_5O_{12}$ and $EuFeO_3$ (R) phases in the Eu_2O_3-Fe_2O_3 system at 1300 and 1400 °C (Figs. 3-5).

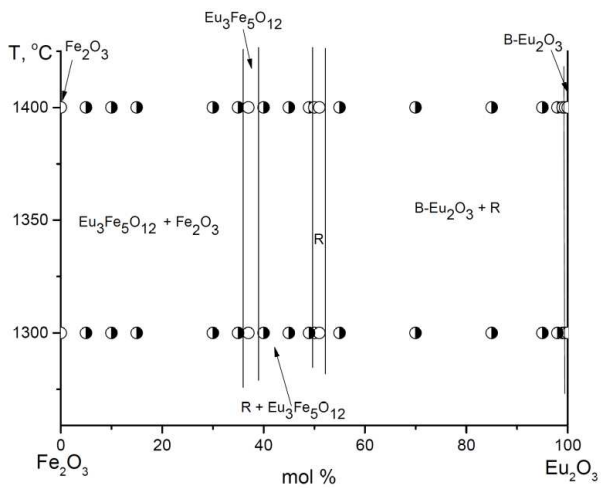

Figure 2. Isothermal sections at 1300 and 1400 °C for the system Fe_2O_3-Eu_2O_3 (○ – single-phase samples, ◑ – two-phase samples)

Table 1. Phase composition and lattice parameters of the phases in the Eu_2O_3-Fe_2O_3 system, annealed at 1300 °C (XRD and SEM data)

Composition [mol%]		Phase composition, parameters of elementary cell [nm]	Parameters of elementary cells of phases [nm] ($a \pm 0.002$)								
Fe_2O_3	Eu_2O_3		R			Fe_2O_3		B-Eu_2O_3			
			a	*b*	*c*	*a*	*c*	*a*	*b*	*c*	*β*
100	0	Fe_2O_3				0.511	1.382				
95	5	Fe_2O_3 + $Eu_3Fe_5O_{12}$ (a = 1.244)				0.503	1.367				
90	10	Fe_2O_3 + $Eu_3Fe_5O_{12}$ (a = 1.247)				0.502	1.374				
85	15	Fe_2O_3 + $Eu_3Fe_5O_{12}$ (a = 1.248)				0.503	1.375				
70	30	Fe_2O_3 + $Eu_3Fe_5O_{12}$ (a = 1.249)									
65	35	Fe_2O_3 + $Eu_3Fe_5O_{12}$ (a = 1.249)									
63	37	$Eu_3Fe_5O_{12}$ (a = 1.248)									
60	40	R + $Eu_3Fe_5O_{12}$ (a = 1.249)									
55	45	R + $Eu_3Fe_5O_{12}$ (a = 1.247)	0.538	0.565	0.777						
51	49	R	0.538	0.559	0.769						
50	50	R	0.538	0.559	0.767						
49	51	R	0.539	0.559	0.768						
45	55	R + B-Eu_2O_3	0.536	0.558	0.767						
30	70	R + B-Eu_2O_3	0.536	0.561	0.768			1.388	0.362	0.873	83.50
15	85	R + B-Eu_2O_3	0.536	0.558	0.768			1.497	0.357	0.890	92.93
5	95	R + B-Eu_2O_3						1.646	0.395	0.880	103.29
2	98	R + B-Eu_2O_3						1.574	0.358	0.888	94.86
1	99	B-Eu_2O_3						1.617	0.359	0.890	96.12
0.5	99.5	B-Eu_2O_3						1.603	0.362	0.889	96.38
0	100	B-Eu_2O_3									

Table 2. Phase composition and lattice parameters of the phases in the Eu_2O_3-Fe_2O_3 system, annealed at 1400 °C (XRD and SEM data)

Composition [mol%]		Phase composition, parameters of elementary cell [nm]	Parameters of elementary cells of phases [nm] ($a \pm 0.002$)								
Fe_2O_3	Eu_2O_3		R			Fe_2O_3		B-Eu_2O_3			
			a	*b*	*c*	*a*	*c*	*a*	*b*	*c*	*β*
100	0	Fe_2O_3				0.511	1.382				
95	5	Fe_2O_3 + $Eu_3Fe_5O_{12}$ (a = 1.251)				0.504	1.375				
90	10	Fe_2O_3 + $Eu_3Fe_5O_{12}$ (a = 1.251)				0.504	1.375				
85	15	Fe_2O_3 + $Eu_3Fe_5O_{12}$ (a = 1.251)									
70	30	Fe_2O_3 + $Eu_3Fe_5O_{12}$ (a = 1.249)									
65	35	Fe_2O_3 + $Eu_3Fe_5O_{12}$ (a = 1.249)									
63	37	$Eu_3Fe_5O_{12}$ (a = 1.248)									
60	40	R + $Eu_3Fe_5O_{12}$ (a = 1.249)									
55	45	R + $Eu_3Fe_5O_{12}$ (a = 1.252)									
51	49	R	0.538	0.564	0.767						
50	50	R	0.538	0.561	0.769						
49	51	R	0.538	0.561	0.769						
45	55	R + B-Eu_2O_3	0.538	0.564	0.767						
30	70	R + B-Eu_2O_3	0.538	0.562	0.770			1.392	0.362	0.842	84.87
15	85	R + B-Eu_2O_3	0.538	0.564	0.770			1.394	0.362	0.869	85.47
5	95	R + B-Eu_2O_3						1.407	0.361	0.864	86.27
2	98	R + B-Eu_2O_3						1.718	0.361	0.893	98.03
1	99	B-Eu_2O_3						1.602	0.357	0.892	94.94
0.5	99.5	B-Eu_2O_3						1.389	0.360	0.853	89.87
0	100	B-Eu_2O_3									

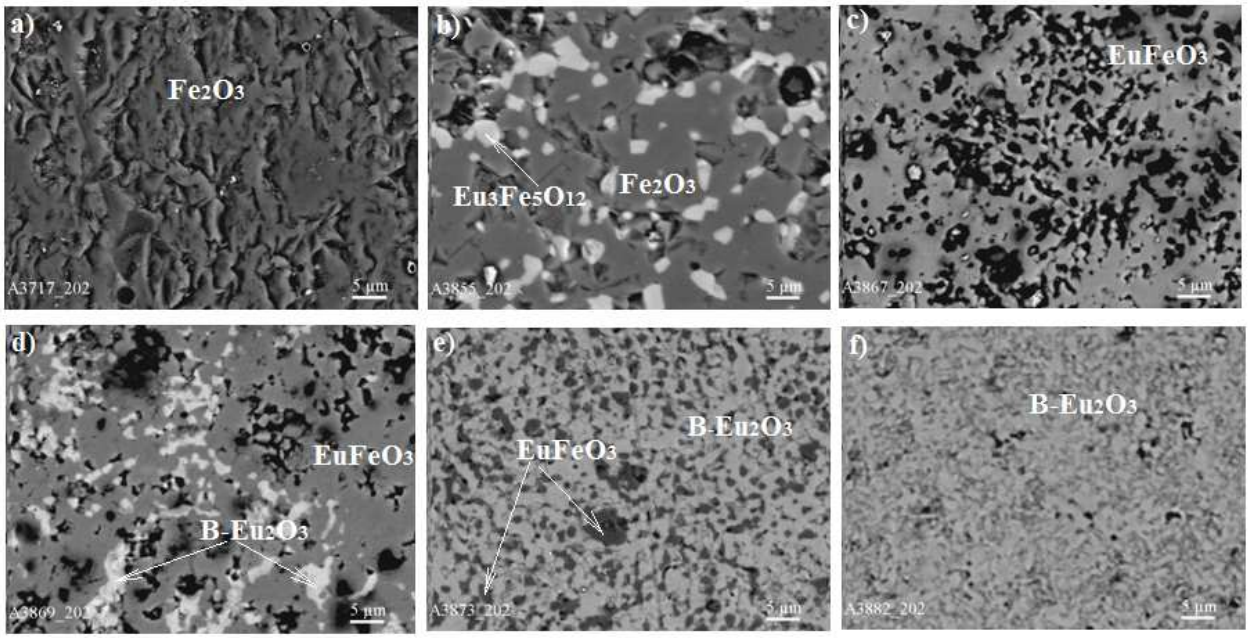

Figure 3. SEM microstructures of the samples in the defined field of compositions of the system Eu_2O_3-Fe_2O_3 heat-treated at 1300 °C: a) 0 mol% Eu_2O_3 - 100 mol% Fe_2O_3, b) 5 mol% Eu_2O_3 - 95 mol% Fe_2O_3, c) 51 mol% Eu_2O_3 - 49 mol% Fe_2O_3, d) 55 mol% Eu_2O_3 - 45 mol% Fe_2O_3, e) 85 mol% Eu_2O_3 - 15 mol% Fe_2O_3, and f) 99 mol% Eu_2O_3 - 1 mol% Fe_2O_3

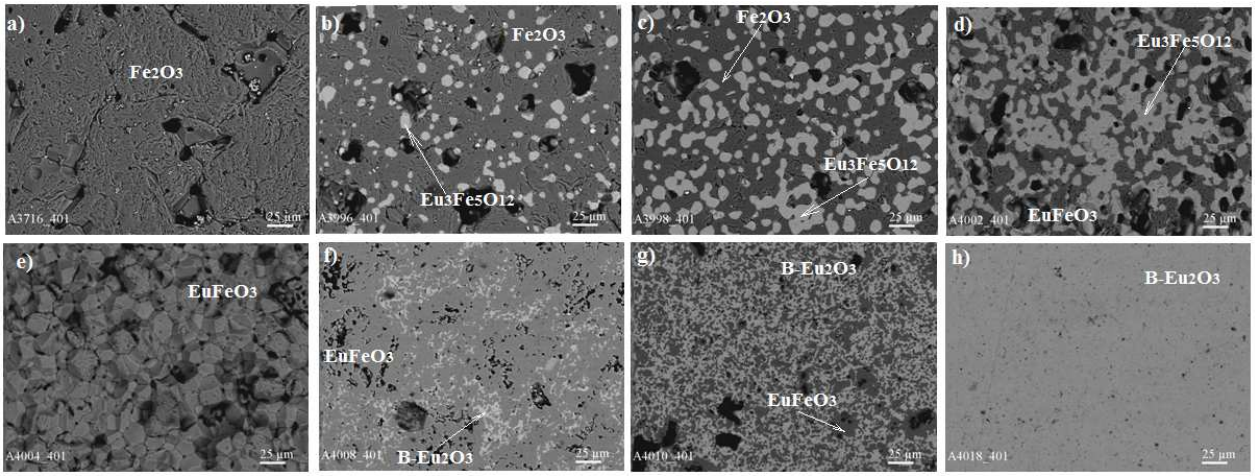

Figure 4. SEM microstructures of the samples in the defined field of compositions of the system Eu_2O_3-Fe_2O_3 heat-treated at 1400 °C: a) 0 mol% Eu_2O_3 - 100 mol% Fe_2O_3, b) 5 mol% Eu_2O_3 - 95 mol% Fe_2O_3, c) 10 mol% Eu_2O_3 - 90 mol% Fe_2O_3, d) 45 mol% Eu_2O_3 - 55 mol% Fe_2O_3, e) 49 mol% Eu_2O_3 - 51 mol% Fe_2O_3, f) 55 mol% Eu_2O_3 - 45 mol% Fe_2O_3, g) 70 mol% Eu_2O_3 - 30 mol% Fe_2O_3 and h) 99 mol% Eu_2O_3 - 1 mol% Fe_2O_3

Figures 3 and 4 present SEM images of the samples after heat treatment at 1300 and 1400 °C, respectively. The pure Fe_2O_3 sample (Figs. 3a and 4a) is characterized by a relatively homogeneous structure with well-defined Fe_2O_3 grains and isolated pores. The microstructure of the 5 mol% Eu_2O_3 - 95 mol% Fe_2O_3 sample (Figs. 4b and 4c) exhibits a two-phase character: the Fe_2O_3 matrix contains uniformly distributed inclusions of the garnet phase $Eu_3Fe_5O_{12}$, which appears as bright grains in the backscattered electron images. With an increasing amount of europium oxide, the fraction of this phase grows and the microstructure becomes finer and more homogeneous. Further phase evolution confirms the formation of a dense and homogeneous perovskite phase, $EuFeO_3$ (Figs. 3c and 4e). The $EuFeO_3$ grains have an isometric shape with clearly defined boundaries, indicating phase stability and the effective formation of the perovskite structure. In the samples containing the monoclinic europium oxide phase (Figs. 3e,f and 4f,g), the microstructure becomes more complex: finely dispersed B-Eu_2O_3 inclusions are observed within the perovskite matrix and evenly distributed throughout the volume. The sample with 99 mol% Eu_2O_3 consisting almost entirely of B-Eu_2O_3 (Fig. 4h), exhibits high homogeneity and a lack of pronounced grain boundaries, indicating the predominant formation of the monoclinic europium oxide phase with minimal impurities. Thus, with increasing europium oxide content in the Eu_2O_3-

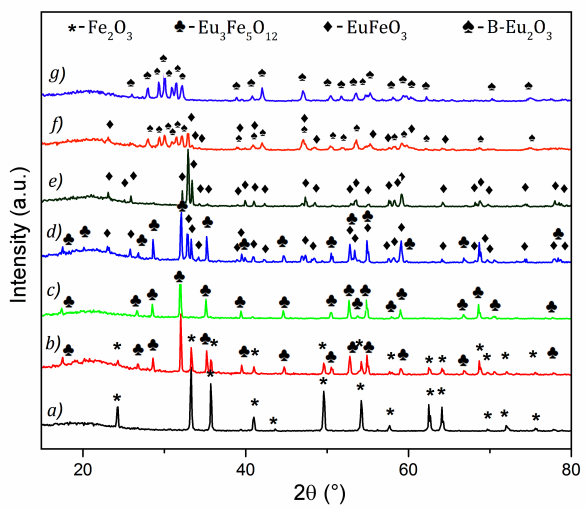

Figure 5. XRD patterns of the samples for the Eu_2O_3-Fe_2O_3 heat-treated at 1300 °C: a) 0 mol% Eu_2O_3 - 100 mol% Fe_2O_3, b) 15 mol% Eu_2O_3 - 85 mol % Fe_2O_3, c) 37 mol% Eu_2O_3 - 63 mol% Fe_2O_3, d) 45 mol% Eu_2O_3 - 55 mol% Fe_2O_3, e) 50 mol% Eu_2O_3 - 50 mol% Fe_2O_3, f) 85 mol% Eu_2O_3 - 15 mol% Fe_2O_3 and g) 99 mol% Eu_2O_3 - 1 mol% Fe_2O_3

Fe_2O_3 system, the microstructure evolves from coarse-grained Fe_2O_3 to fine-grained $EuFeO_3$ and B-Eu_2O_3 phases. The incorporation of europium oxide leads to a reduction in grain size and enhanced microstructural uniformity, which can significantly influence the physicochemical properties of the material.

In the system Eu_2O_3-Fe_2O_3 at 1300 and 1400 °C, an ordered phase of perovskite-type with rhombic distortion was revealed. For the first time, a region of homogeneity for the ordered $EuFeO_3$ (R) phase was established at 1300 and 1400 °C, extending from 49 to 52 mol% Eu_2O_3, Figs. 6a-c. The lattice parameters of the unit cell for R phase vary from a = 0.536 nm, b = 0.561 nm, c = 0.768 nm in the two-phase sample (B + R), containing 70 mol% Eu_2O_3, to a = 0.538 nm, b = 0.559 nm, c = 0.769 nm for the solid solution of the boundary composition, in the sample containing 49 mol% Eu_2O_3 (Table 1, Fig. 5).

It should be noted that in the Fe_2O_3-La_2O_3 and Fe_2O_3-Nd_2O_3 systems at 1300 and 1400 °C, the perovskite phase has a clearly defined stoichiometric composition, not a region [17,18].

For the first time, a region of homogeneity for the ordered $Eu_3Fe_5O_{12}$ phase was established at 1300 and 1400 °C, extending from 61 to 63 mol% Fe_2O_3 (Fig. 7). The lattice parameter of the unit cell $Eu_3Fe_5O_{12}$ phase varies from a = 1.249 nm in the two-phase samples ($Eu_3Fe_5O_{12}$ + Fe_2O_3 and $Eu_3Fe_5O_{12}$ + R, containing 35 mol% Eu_2O_3 - 65 mol% Fe_2O_3 and 40 mol% Eu_2O_3 - 60 mol% Fe_2O_3, respectively) to a = 1.248 nm in the single-phase sample for the composition containing 37 mol% Eu_2O_3 and 63 mol% Fe_2O_3 (Table 1, Fig. 5). In the Fe_2O_3-Nd_2O_3 system at 1300 and 1400 °C, the cubic phase of the $Ln_3Fe_5O_{12}$ type phase does not form [18].

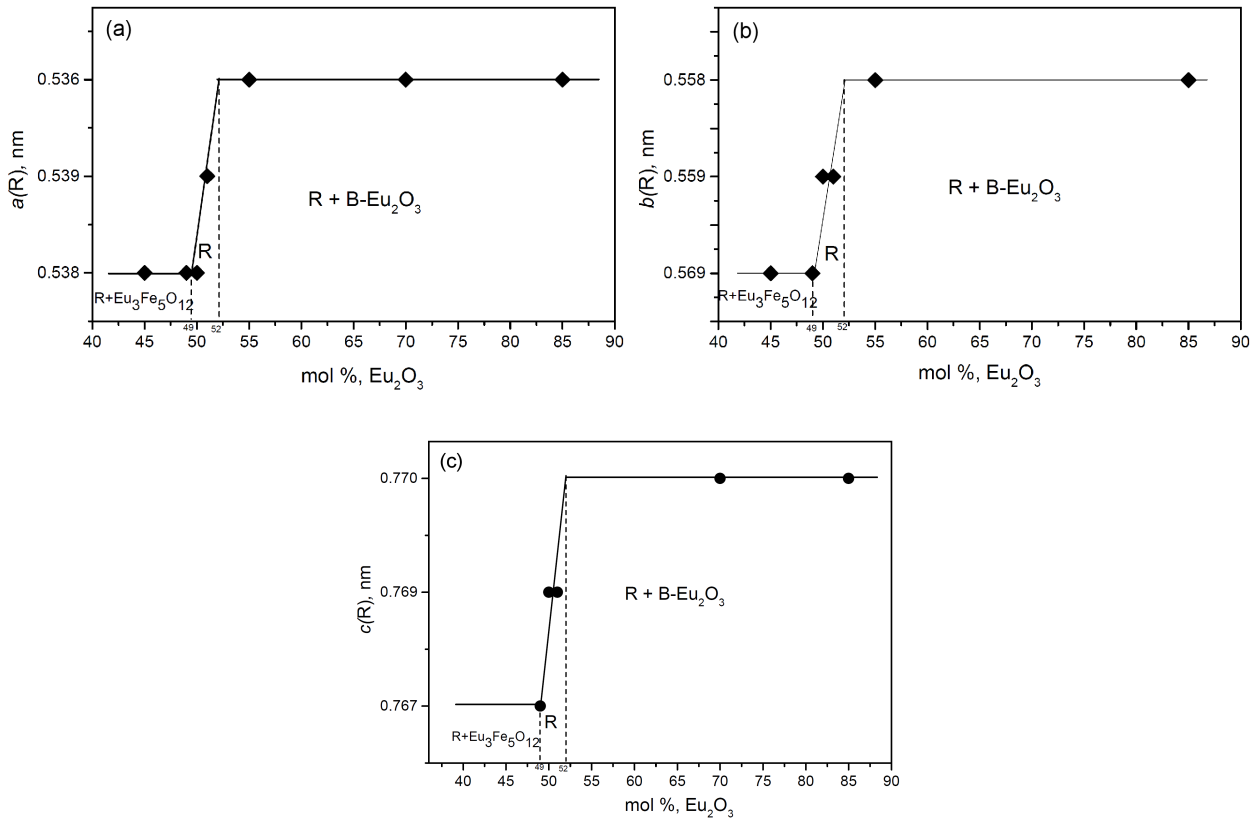

Figure 6. Concentration dependence of lattice parameters for solid solutions based on on the $EuFeO_3$ (R) phase in the system Eu_2O_3-Fe_2O_3 heat-treated at 1300 °C (a, b) and 1400 °C (c)

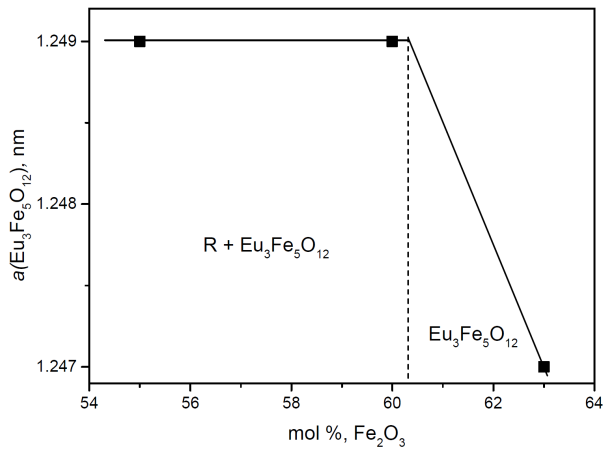

Figure 7. Concentration dependence of lattice parameters for solid solutions based on $Eu_3Fe_5O_{12}$ in the system Eu_2O_3-Fe_2O_3 heat-treated at 1300 °C

Europium oxide forms solid solutions based on the monoclinic modification. Using the concentration dependences of the unit cell parameters, it was established that the range of homogeneity of solid solutions based on the B-phase extends from 99 to 100 mol% Eu_2O_3 at 1300 and 1400 °C, Tables 1 and 2. The lattice parameters of the unit cell B-Eu_2O_3 phase vary from a = 1.574 nm, b = 0.395 nm, c = 0.888 nm, β = 94.86° in the two-phase samples (B-Eu_2O_3 + R, containing 98 mol% Eu_2O_3) to a = 1.617 nm, b = 0.359 nm, c = 0.890 nm, β = 96.12° in the single-phase sample containing 99 mol% Eu_2O_3 (Table 1). The Fe_2O_3 does not form regions of homogeneity (Fig. 2, Tables 1 and 2).

IV. Conclusions

Phase equilibria were studied in the Eu_2O_3-Fe_2O_3 system at 1300 and 1400 °C. It has been established that solid state interactions between two oxides resulted in the formation of phases (B-Eu_2O_3, $EuFeO_3$, $Eu_3Fe_5O_{12}$, Fe_2O_3). The homogeneity region of the ordered phase $EuFeO_3$ (R) at 1300 and 1400 °C has been bound by compositions from 49 to 52 mol% Eu_2O_3. The boundaries of the homogeneity region of the ordered phase $Eu_3Fe_5O_{12}$ at 1300 and 1400 °C fall in the region of 61–63 mol% Fe_2O_3. The range of homogeneity of solid solutions based on the B-phase extends from 99 to 100 mol% Eu_2O_3 at 1300 and 1400 °C. The thermal stability of the phases in the range of 1300–1400 °C makes them promising for applications in the high-temperature electronics, catalysis and protective coatings. The results obtained provide a basis for the synthesis of new functional materials with controlled magnetic and optical properties, enabling their potential use in optoelectronics, magneto-optics, and spintronics.

Acknowledgement: This work supported by the research project of the NAS of Ukraine "New photocatalytic materials based on perovskite-type phase".

References

1. J. Pilo, E.P. Arévalo-López, J.M. Cervantes, R. Escamilla, M. Romero, "DFT+U study of the structural, electronic and magnetic properties in the $EuCoO_3$, $EuFeO_3$, and $EuCo_{0.5}Fe_{0.5}O_3$ type perovskite compounds", *J. Magn. Magn. Mater.,* **589** (2024) 171543.
2. P. Tang, H. Chen, C. Lv, K. Wang, Y. Wang, "Microwave synthesis of nanoparticulate $EuFeO_3$ and its visible light photocatalytic activity", *Integr. Ferroelectr.*, **181** [1] (2017) 49–54.
3. F. Sayetat, "Huge magnetostriction in $Tb_3Fe_5O_{12}$, $Dy_3Fe_5O_{12}$, $Ho_3Fe_5O_{12}$, $Er_3Fe_5O_{12}$ garnets", *J. Magn. Magn. Mater.*, **58** [3-4] (1986) 334–346.
4. M. Ristić, M. Ristić, I. Nowik, S. Popović, S. Musić "Formation of oxide phases in the system Eu_2O_3-Fe_2O_3", *Croat. Chem. Acta*, **73** [2] (2000) 525–540.
5. T.V. Aksenova, N.E. Volkova, L.Ya. Gavrilova, V.A. Cherepanov, "Phase equilibria, crystal structure and oxygen nonstoichiometry of complex oxides in the ½Eu_2O_3–SrO–½Fe_2O_3 system", *J. Alloys Compd.,* **1036** (2025) 182000.
6. M. Drofenik, D. Kolar, L. Golič, "Phase relation in the system SrO-Eu_2O_3-Fe_2O_3 and a new ternary phase $S_{r2}EuFe_{O5}$", *J. Less Common Met.*, **37** (1974) 281–284.
7. G.J. McCarthy, R.D. Fischer, "The system Eu-Fe-O compound formation and its implications for systematic crystal chemistry", *J. Solid State Chem.*, **4** (1972) 340–344.
8. S.C. Parida, S.K. Rakshit, S. Dash, Ziley Singh, R. Prasad, V. Venugopal, "Systems Ln-Fe-O (Ln = Eu, Gd): thermodynamic properties of ternary oxides using solid-state electrochemical cells", *J. Solid State Chem.*, **172** (2003) 370–380.
9. M. Ristić, S. Popović, S. Czakó-Nagy, Musić, "Formation and characterization of oxide phases in the Fe_2O_3-Eu_2O_3 system", *Mater. Lett.*, **27** (1996) 337–341.
10. T. Sugihara, N. Kimizuka, T. Katsura,"Phase equilibria in the Fe-Fe_2O_3-Eu_2O_3 System at 1200 °C", *Bull. Chem. Soc. Jpn.,* **48** [6] (1975) 1806–1808.
11. V.S. Kuzmin, V.M. Kolesenko, "Amplitude dependence of single-pulse nuclear echo in $Eu_3Fe_5O_{12}$ ferrimagnetic", *J. Appl. Spectrosc.*, **79** (2012) 390–397.
12. M.K. Warshi, V. Mishra, A. Sagdeo, V. Mishrad, R. Kumara, P.R. Sagdeo, "Structural, optical and electronic properties of $RFeO_3$", *Ceram. Int.*, **44** (2018) 8344–8349.
13. L. Boudad, M. Taibi, A. Belayachi, M. Abd-Lefdil, "Structural, morphological, thermal, and oxygen-vacancy-related dielectric relaxation behaviors in $EuFeO_3$ perovskite", *Mater. Today. Proc.*, **58** (2022) 1028–1032.
14. X. Niu, H. Li, G. Liu, "Preparation, characterization and photocatalytic properties of $REFeO_3$ (RE = Sm, Eu, Gd)", *J. Mol. Catal. A Chem.*, **232** (2005) 89–93.
15. S. Huang, K.P. Su, H.O. Wang, S.L. Yuan, D.X. Huo, "High temperature dielectric response in $R_3Fe_5O_{12}$ (R = Eu, Gd) ceramics", *Mater. Chem. Phys.*, **197** (2017) 11–16.
16. O. Opuchovic, A. Kareiva, K. Mazeika, D. Baltrunas, "Magnetic nanosized rare earth iron garnets $R_3Fe_5O_{12}$: Sol-gel fabrication, characterization and reinspection", *J. Magn. Magn. Mater.*, **422** (2017) 425–433.
17. O.V. Chudinovych, D.V. Vedel, O.O. Stasyuk, T.V. Tomila, M.H. Aguirre, "Production, structure and magnetic properties of nanocomposites based on the perovskite phase $LaFeO_3$", *Solid State Sci.*, **157** (2024) 107699.
18. O.V. Chudinovych, D.V. Vedel, O.O. Stasyuk, A.V. Same-

lyuk, M.H. Aguirre, "Phase relations in the Nd_2O_3-Fe_2O_3 system: Structure andmagnetic properties of perovskite $NdFeO_3$ ceramics", *Process. Appl. Ceram.*, **18** [3] (2024) 314–322.